

Ion kinetic energy spectroscopy of the doubly charged ion of carbon monoxide

J. M. Curtis and R. K. Boyd

Citation: [The Journal of Chemical Physics](#) **80**, 1150 (1984); doi: 10.1063/1.446844

View online: <http://dx.doi.org/10.1063/1.446844>

View Table of Contents: <http://scitation.aip.org/content/aip/journal/jcp/80/3?ver=pdfcov>

Published by the [AIP Publishing](#)

Articles you may be interested in

[Thermochemistry and energy partitioning in the charge separation reactions of doubly charged triatomic ions](#)

J. Chem. Phys. **61**, 1208 (1974); 10.1063/1.1681995

[Metastable Dissociation of the Doubly Charged Carbon Monoxide Ion](#)

J. Chem. Phys. **53**, 132 (1970); 10.1063/1.1673756

[Metastable State of the Doubly Charged Carbon Dioxide Ion](#)

J. Chem. Phys. **40**, 718 (1964); 10.1063/1.1725195

[Kinetics of the Alpha Radiolysis of Carbon Monoxide](#)

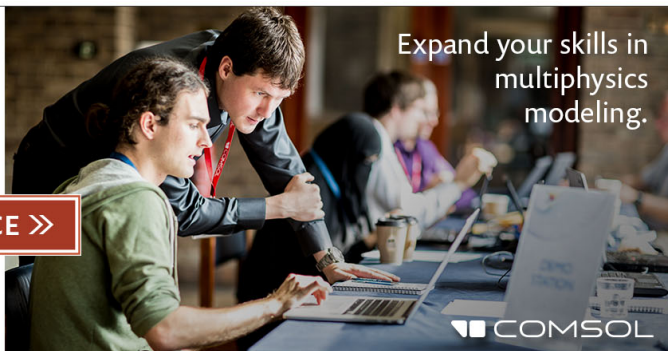
J. Chem. Phys. **33**, 705 (1960); 10.1063/1.1731242

[Dissociation Energy of Carbon Monoxide](#)

J. Chem. Phys. **24**, 1103 (1956); 10.1063/1.1742688

Ready, set, simulate.

REGISTER FOR THE COMSOL CONFERENCE »



Ion kinetic energy spectroscopy of the doubly charged ion of carbon monoxide

J. M. Curtis and R. K. Boyd

Guelph-Waterloo Centre for Graduate Work in Chemistry, University of Guelph, Guelph, Canada N1G 2W1

(Received 17 August 1983; accepted 28 October 1983)

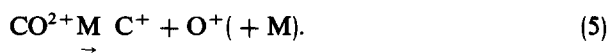
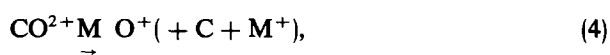
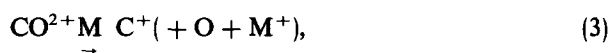
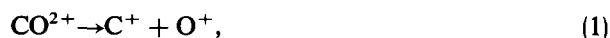
Spontaneous and collision-induced dissociation processes of CO^{2+} ions, formed by electron impact, have been studied in a double-focusing mass spectrometer using techniques of ion kinetic energy spectroscopy. The predissociation process, responsible for unimolecular dissociation of CO^{2+} on the microsecond time scale, is almost certainly electronically adiabatic tunneling through a potential barrier, though predissociation via electronic curve crossing cannot be entirely ruled out. Semiempirical potential curves for states of CO^{2+} were revised in order to better accommodate all of the available data, including Auger spectra, appearance energies, and kinetic energy release. Collision induced dissociation processes with Ar, N_2 , and H_2 proceed via charge exchange, and involve predissociation of the $D^2\Pi$ state by the $C^2\Delta$ state of CO^+ . When He is used as collision gas, the dissociation processes involving charge exchange are different, and require an energetic contribution from the relative kinetic energy (kinetic energy loss). In addition, He is quite different in inducing dissociation of CO^{2+} without prior charge exchange, from states of CO^{2+} up to 13 eV above the dissociation limit.

INTRODUCTION

The spontaneous decomposition of doubly charged diatomic ions, on the time scale of processes occurring in field-free regions of magnetic sector mass spectrometers (a few microseconds), is a phenomenon which has been studied for over 50 years. In 1932, Friedlander *et al.*¹ observed, in the mass spectrum of CO, conventional metastable peaks corresponding to fragmentation of CO^{2+} to C^+ and O^+ . These authors,¹ however, reported an intensity for the O^+ fragment ion about 30 times that for the C^+ fragment. In 1948, Hipple² reported unsuccessful separate attempts by Fox and by Dibeler to repeat the original work. This led Melton and Wells³ to investigate whether or not the process might be collision induced; the discrepancies described above might then be due to different background pressures in the mass spectrometer analyzer. In fact, Melton and Wells³ did observe a collision-induced fragmentation of CO^{2+} , leading predominantly to C^+ (plus O neutral) consistent with a charge-exchange mechanism, but were unable to observe a spontaneous fragmentation at all.

All of these earlier studies¹⁻³ were similar in that they used single-focusing mass spectrographs¹ or mass spectrometers^{2,3} with a single magnetic analyzer. The signals arising from the various fragmentation processes, as well as the main-beam mass spectrum corresponding to ions formed in the ion source, thus all overlap with one another. These difficulties did not apply to the work of Kupriyanov,⁴ who used two magnetic sectors in tandem, with differential pumping of the various regions of the instrument, and an enclosed collision chamber between the two analyzers. Mass-selected ions were transmitted by the first sector, and their spontaneous and collision-induced reactions studied via the momentum spectra provided by the second analyzer. In this way it

was possible to show⁴ that all of the following processes occur:



Process (1) is the true unimolecular fragmentation of CO^{2+} , while process (5) is its collision-induced counterpart. Processes (3) and (4) are the collision-induced fragmentation processes proceeding via charge exchange, as observed previously,³ while process (2) is the corresponding charge-exchange process (20/11 process in the notation of Hasted⁵) occurring without fragmentation. The relative efficiencies of the various processes depended⁴ upon the nature of the collision gas M. The values of the kinetic energy release in processes (1) and (5) are shown, in the present work, to be much larger than for processes (3) and (4); this may have contributed to the confusion in the results of the earlier investigators.

A more recent investigation of this type was due to Newton and Sciamanna⁶ who were able to study the unimolecular process (1) in a Dempster-type mass spectrometer and to provide the first measurement (5.75 ± 0.2 eV) of the associated kinetic energy release. These workers⁶ also showed that the appearance energies of CO^{2+} which survived to the detector, and of the C^+ and O^+ products from metastable CO^{2+} , were indistinguishable within the range

41.5 ± 0.4 eV. Finally, on the basis of two different experimental procedures, the half-life of CO^{2+} was found⁶ to lie in the range 15 to 30 μs , and no CO^{2+} of effectively infinite lifetime was detected.⁶ The most reliable value of the kinetic energy release, presently in the literature, is the value 5.6 ± 0.1 eV obtained by Beynon *et al.*⁷ using techniques essentially identical to those used in the present work.

The theoretical interpretation of these observations is based upon the form of the potential energy curves for CO^{2+} , as first described qualitatively by Dorman and Morrison.⁸ For states correlating with two singly charged atomic ions at the dissociation limit, the combination of an attractive potential well with a Coulombic repulsion curve can lead to a net potential energy curve in which a potential energy maximum separates the well from the dissociation limit, even for zero angular momentum.⁸ (The centrifugal barrier in states with $J > 0$ would add to the intrinsic barrier corresponding to the $J = 0$ curve.) The observed spontane-

ous dissociation of CO^{2+} could then correspond to rotation-vibrational states of CO^{2+} , of appropriate lifetime, tunneling through this potential barrier. Since the proposed process is electronically adiabatic, it corresponds to Herzberg's predissociation case III mechanism,⁹ even though the barrier is not entirely rotational in origin. No information concerning electronic states of CO^{2+} is available from optical spectroscopy.^{9,10} Hurley^{11,12} has developed an ingenious semiempirical procedure for relating potential energy curves of doubly charged diatomics to those of isoelectronic neutral diatomics. The appropriate neutral species for CO^{2+} is BN, and two states of this species have been well characterized spectroscopically.^{7,8} Unfortunately the dissociation energy of the $X^3\Pi$ ground state of BN is uncertain. A linear Birge-Sponer extrapolation of the observed progression^{7,8} yields $D_0(\text{BN}) = 5.8$ eV, but Gaydon¹³ favors a value of 4.0 ± 0.5 eV based upon a nonlinear extrapolation. Some rather early thermochemical data suggest $D_0(\text{BN}) > 4.93$ eV, and this has led Herzberg⁹ to tentatively assign a value of 5.0 eV. Using this value, Hurley¹² constructed potential energy curves for two states ($X^3\Pi$ and $A^3\Pi$) of CO^{2+} , and evaluated energies and lifetimes of the vibrational levels for the zero angular momentum case. On this basis Hurley¹² was able to reconcile the observations of Newton and Sciamanna,⁶ which seemed to demand a ground electronic state of CO^{2+} sufficiently shallow as to support only one vibrational level, with the observation by high resolution Auger spectroscopy¹⁴ of what appears to be a vibrational progression (containing at least 6 lines) in the ground state of CO^{2+} . Hurley's curve¹² is drawn in Fig. 1, together with known data on the states of CO^+ . We shall return later to the dilemma addressed by Hurley,¹² and also to a more complete discussion of the states of CO^+ .

The objective of the present work was to investigate processes (1)–(5) in a modern double-focusing mass spectrometer, using techniques of ion kinetic energy spectroscopy.¹⁵ In addition, more recent information on states of CO^+ and CO^{2+} will be considered in attempting to provide a self-consistent account of all available data.

II. EXPERIMENTAL

All of the data reported here were obtained using a VG7070F double-focusing mass spectrometer. This instrument is equipped with a conventional Nier-type source, with the nominal electron energy continuously variable in the range 5 to 105 eV. Unless stated otherwise, all experiments reported here used a nominal electron energy of 70 eV, and an ion source temperature of 200 °C. The usual accelerating voltage is 4 kV, and the energy spread of the main beam is typically 1.5 eV, so the inherent energy resolution is of the order of 2500. However, in practice the limits on kinetic energy resolution are set by the angular acceptance of the ion optics; installation of special apertures to collimate the beam is not feasible on this instrument, which is in daily use to provide an analytical service. The instrument is equipped with a fully closeable energy resolving (beta) slit, which for ion kinetic energy spectroscopy experiments was set narrow enough that the energy resolution was not limited by slit widths.

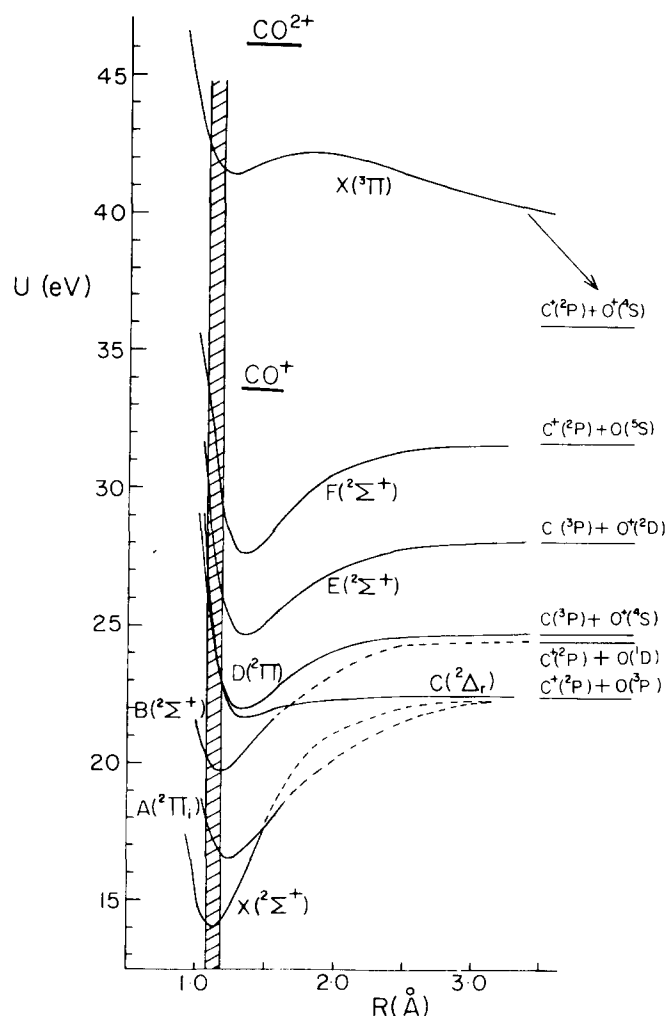


FIG. 1. Potential energy curves for states of CO^+ and of CO^{2+} . The heavy curves for the X , A , and B States of CO^+ are RKR potentials (Ref. 44), and their dash extensions are approximate curves showing the appropriate dissociation limits. The curve for the $C^2\Delta$ state is a Morse curve generated using experimentally derived constant (Ref. 33). The D , E , and F states are discussed in the text. The $X^3\Pi$ state of CO^{2+} is the semiempirical curve given previously (Ref. 11). The vertical shaded region shows the Franck-Condon region for transitions from the $v = 0$ level of the $X^1\Sigma^+$ state of CO .

The instrument is differentially pumped. The ion gauge located in the ion source housing indicated a pressure $< 8 \times 10^{-8}$ Torr in the absence of a sample. CO was admitted to the source until this gauge indicated 10^{-6} Torr; at this condition, the ion gauge situated between the electric sector housing and its diffusion pump indicated 1.5×10^{-8} Torr. Collision gas can be admitted through a leak valve to a small enclosed region situated immediately after the first optical slit (ion source slit); this collision gas is preferentially pumped to the analyzer side, and the pressure ratio, between the gas inside this collision cell and that in the main analyzer, is about 100:1.

The ion kinetic energy spectra were mostly obtained using the technique of scanning the accelerating voltage, first described by Barber and Elliott.¹⁶ Some $2E$ spectra¹⁵ were also obtained, to observe process (2); such spectra are obtained by a simple magnet scan, but with the electric sector field held at double the value normally used in the double-focusing mode.¹⁵ The carbon monoxide was obtained from Matheson Co.; it was stated to be of 99.5% purity, and was used as received. No impurities were detected by mass spectrometry, other than those expected from the air background. The collision gases used (N_2 , Ar, He, and H_2) were also used as received from Matheson.

III. RESULTS

The ion kinetic energy spectrum corresponding to process (1), obtained by scanning the accelerating voltage with the magnet set to transmit O^+ fragment ions, is shown in Fig. 2. A similar spectrum was obtained with the magnet set to transmit C^+ fragment ions. The lower intensity of one "horn" reflects a greater degree of ion-source detuning on scanning V . The general form of the spectrum due to spontaneous fragmentation of CO^{2+} is typical¹⁵ of a fragmentation with a large value of kinetic energy release T , the center of the peak being greatly reduced in intensity due to z discrimination. (The z direction is defined here as the direction of the magnetic field, which is also the "slit-height" direction). The values of kinetic energy release, calculated from the widths

between the two sharp horns in each case, agree for C^+ and O^+ fragments at $T = 5.3 \pm 0.1$ eV. The positions of these horns are in general somewhat dependent upon the degree of z discrimination imposed by the instrument used.¹⁵ However, in the present case the very sharp rise of the outside extremities of the peak is characteristic¹⁵ of a single-valued kinetic energy release (or of a very narrow distribution), so that the present value for T is probably not subject to any great uncertainty from this source. The present result is in only moderate agreement with the previous⁶ value of 5.75 ± 0.2 eV. However, the latter value⁶ was measured by a retardation technique, of uncertain accuracy, and the discrepancy could reflect this uncertainty.

It is of interest that, in the present work, the maximum signal for the O^+ fragment ion was consistently about double that for the C^+ fragment, for the spontaneous fragmentation of CO^{2+} . This is far less than the factor of ~ 30 reported previously,¹ but is in the same direction. At least in the present case, it is felt that the discrepancy is probably due to greater collection efficiency for the heavier O^+ (same c.m. momentum, so a smaller transverse velocity), and possibly also to different efficiencies in creating secondary electron emission at the first dynode of the multiplier. The reasons for this difference are not entirely clear.

However, the collision-induced peak for C^+ formed from CO^{2+} , Fig. 3, appeared on introduction of collision gas while leaving the intensity of the unimolecular peak essentially unaltered, though the peak was somewhat broadened. The collision-induced peak is shown considerably expanded in Fig. 4, where the structure in the peak is clearly visible. The structure is symmetrical about the central value of $V/V_0 = 1.167$ corresponding to $\text{CO}^{2+} \rightarrow \text{C}^+$. The values of kinetic energy release corresponding to the three pairs of structure peaks closest to the intense central peak are 0.15 ± 0.02 , 0.31 ± 0.04 , and 0.48 ± 0.06 eV. These have the appearance of a vibrational progression. Use of Ar, or of H_2 , instead of N_2 as collision gas, yield identical results so the observed structure is characteristic of the ion. The corresponding scan for the O^+ fragment shows an extremely weak collision-in-

COMPLETE UNIMOLECULAR PEAK
 $\text{CO}^{2+} \rightarrow \text{O}^+$

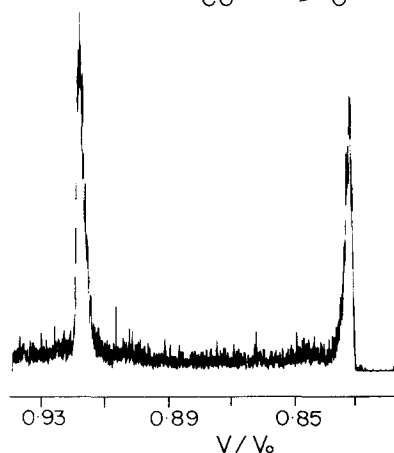


FIG. 2. Ion kinetic energy spectrum for unimolecular dissociation process $\text{CO}^{2+} \rightarrow \text{O}^+$.

$\text{CO}^{2+} \rightarrow \text{C}^+$ COMPLETE UNIMOLECULAR PEAK (a)
AND CENTRAL N_2 C.I.D. PEAK (b)

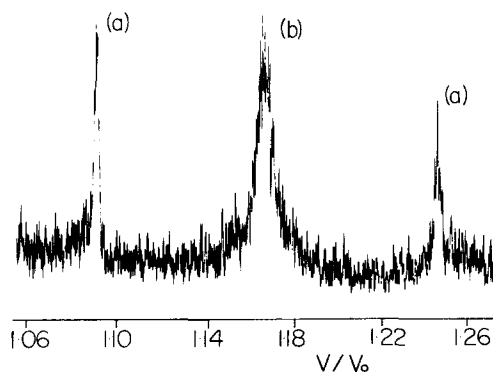


FIG. 3. Ion kinetic energy spectrum for $\text{CO}^{2+} \rightarrow \text{C}^+$, both unimolecular (a) (horns at extremities of spectrum) and collision induced (b) by collisions with N_2 (structured peak at center).

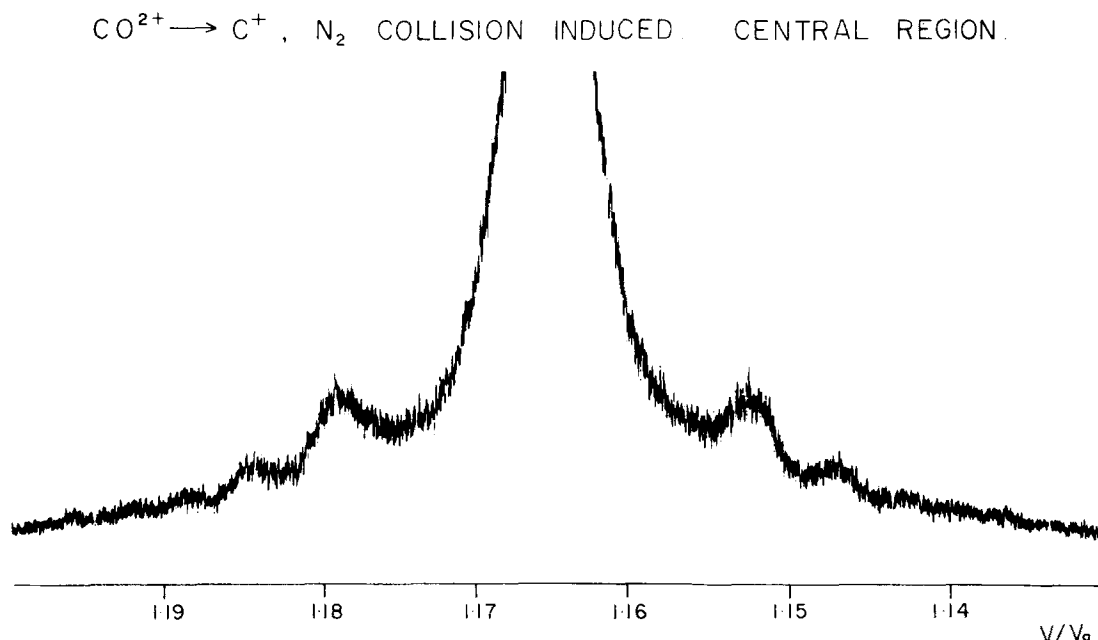


FIG. 4. Expanded version of central portion of Fig. 3, showing ion kinetic energy spectrum for $\text{CO}^{2+} \rightarrow \text{C}^+$ induced by collisions with N_2 .

duced peak if the collision gas is Ar, N_2 , or H_2 (see Fig. 8, for example). The case of He as collision gas is described below. The relatively small values of kinetic energy release (Fig. 4), together with the observed predominance of C^+ fragments over O^+ fragments, suggests that Ar, N_2 , and H_2 act as charge-exchange gases in process (2), with subsequent fragmentation of some of the CO^+ thus formed. [The energetics of process (3) are more favorable than those of process (4) as discussed below]. A series of $2E$ experiments,¹⁵ designed to detect unfragmented CO^+ formed by process (2), showed that each of Ar, N_2 , and H_2 were about equally efficient, and at least an order of magnitude more efficient than He.

Among the collision gases used in the present work, helium stands somewhat apart from the rest. For example, Fig. 5 contrasts the effect of He collision gas on the peak corresponding to process (1) with that of N_2 . Only one of the horns was recorded for Fig. 5, since it was difficult to maintain the magnetic field constant, to within the required accuracy, for the length of time required for the slow scan used; the other horn (not shown) was the mirror image of Fig. 5. There is clear evidence of process (5) occurring from CO^{2+} states of higher energy, reached via a collision with He. Figure 5 shows that N_2 also can effect this excitation, but with very low efficiency such that the extra peak is barely discernible.

The corresponding effect for the O^+ fragment (Fig. 6) illustrates this point even more closely. The baseline is much more clean in the absence of collision gas than is the corresponding C^+ case (Fig. 5), because the O^+ ions detected here have higher values of (kinetic energy/charge) than does the main beam of singly charged ions. Thus there is no interference from low energy background ions formed in processes such as $AB^+ \rightarrow A^+ + B$, occurring in various regions of the instrument as described by Lacey and Macdonald.¹⁷

Helium collision gas was also observed to induce processes (3) and (4), presumably via process (2). However, the efficiency of He, in inducing formation of C^+ via process (3),

was at least an order of magnitude less than that of any Ar, H_2 , or N_2 . In addition, as illustrated in Fig. 7, the nature of the process appears to be significantly different. Thus Fig. 7 shows no evidence of the regular structure (Fig. 4), and it

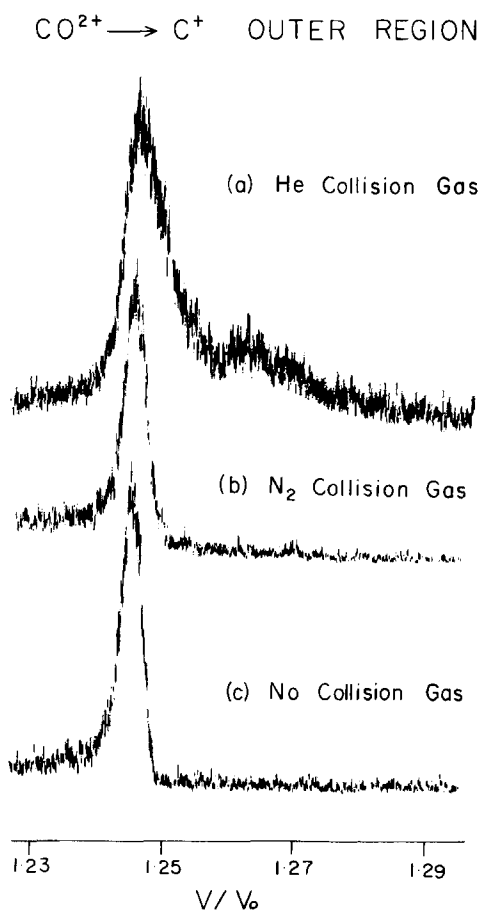


FIG. 5. Low energy side (high V/V_0) of ion kinetic energy spectrum for $\text{CO}^{2+} \rightarrow \text{C}^+$ with high values of kinetic energy release. (a) Helium collision gas; (b) nitrogen collision gas; (c) no collision gas used.

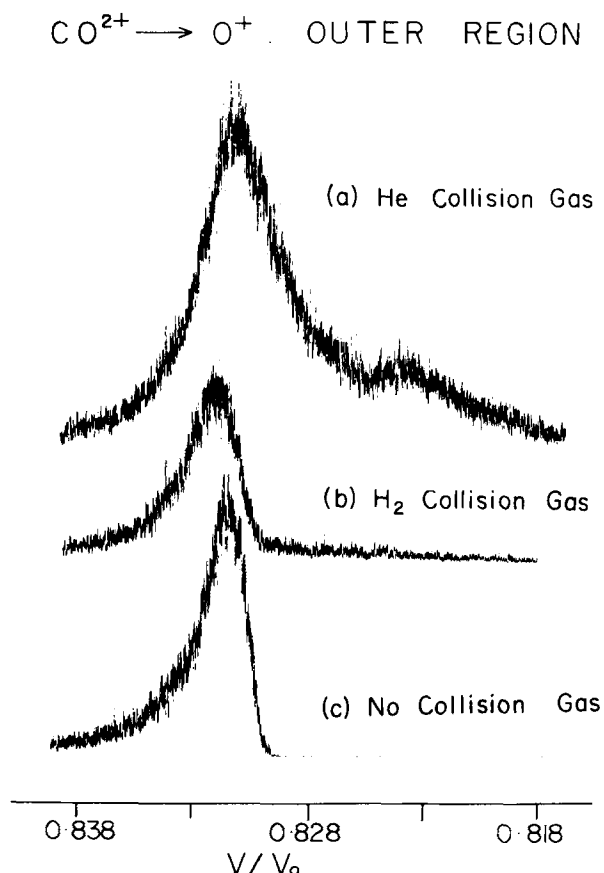


FIG. 6. High energy side (low V/V_0) of ion kinetic energy spectrum for $\text{CO}^{2+} \rightarrow \text{O}^+$ with high values of kinetic energy release. (a) Helium collision gas; (b) hydrogen collision gas; (c) no collision gas used (c.f. Fig. 5).

does appear as if Fig. 7 contains two peaks, one slightly displaced from the other. The available signal-to-noise ratio is too low for any reliable measurements of kinetic energy loss to be made, but the asymmetric character of the peak was reproducible.

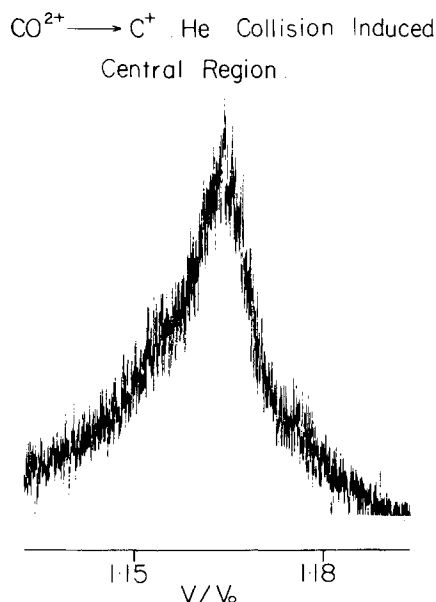


FIG. 7. Ion kinetic energy spectrum for $\text{CO}^{2+} \rightarrow \text{C}^+$ with low values of kinetic energy release, induced by collisions with helium.

In contrast, as illustrated in Fig. 8, helium was found to be much more efficient than any other of the collision gases investigated in inducing formation of O^+ fragments via process (4) [again presumably via process (2)]. The structure evident in Fig. 4 is absent, the peak is perfectly symmetrical within the uncertainties apparent in Fig. 8, and the collision efficiency is appreciably higher than that for process (3) with helium (Fig. 7). The other collision gases were far less efficient than helium in this respect (Fig. 8).

A few experiments, both without collision gas and with either N_2 or He collision gas, were performed using an ion source temperature of 375°C . No significant differences, within the available resolution and sensitivity, could be seen between these spectra and those obtained using an ion source temperature of 200°C . Further, the intensities of all the collision-induced peaks shown in Figs. 3–9 were shown to increase linearly with collision gas pressure, and to extrapolate to zero intensity at zero pressure to within experimental uncertainty.

Appearance energies were estimated for several of the processes observed. Apart from the usual uncertainties arising from use of an unfiltered electron beam from a hot tungsten filament, the intrinsically low intensities of most of the processes observed prevented a high degree of accuracy from being attained. The results obtained are shown in Fig. 9, plotted as the square root of intensity vs nominal electron energy. The latter scale was calibrated against a value of 41.6 eV for the appearance energy of the CO^{2+} ion itself. This value represents the average of four independent determinations by electron impact methods,^{6,8,18,19} and appears to be reproducible to within ± 0.3 eV. In accordance with previous findings,⁶ the appearance energies of the metastable peaks, corresponding to process (1), could not be distinguished from that of CO^{2+} ions which survived to the detector. This was also found to be true for the collision-induced

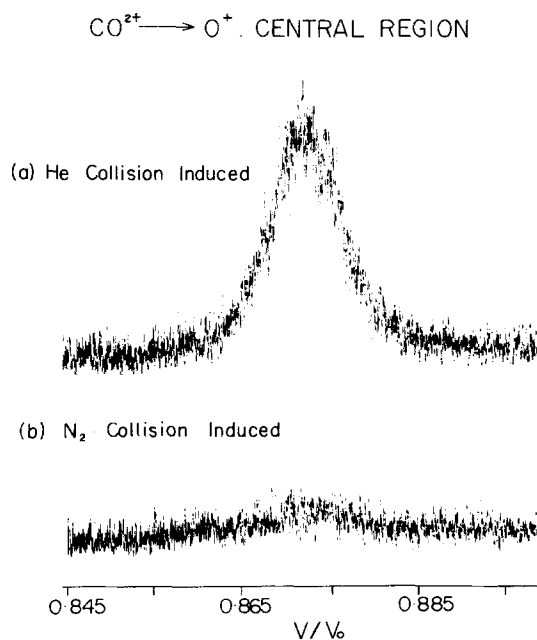


FIG. 8. Ion kinetic energy spectrum for $\text{CO}^{2+} \rightarrow \text{O}^+$ with low values of kinetic energy release, induced by collisions with (a) helium; (b) nitrogen.

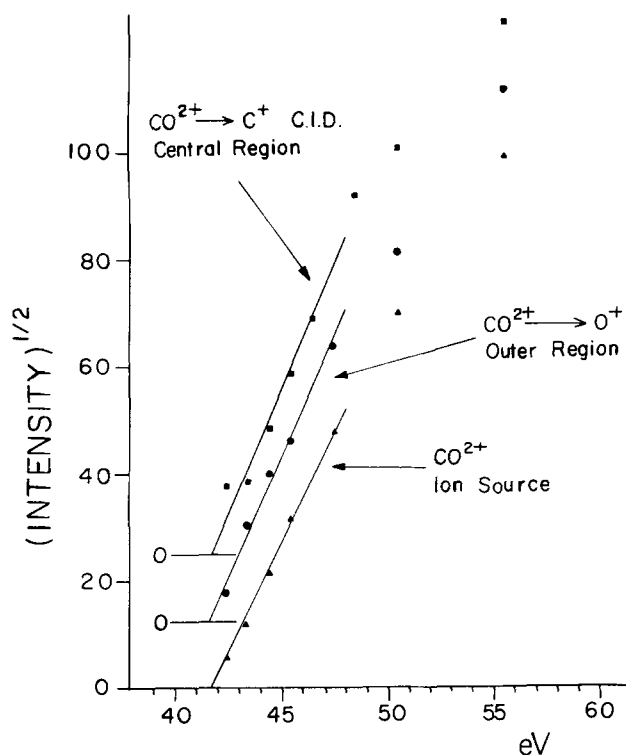


FIG. 9. Appearance energies for CO^{2+} stable on mass spectrometer time scale (used as energy reference), for the $\text{CO}^{2+} \rightarrow \text{O}^+ (+ \text{C}^+)$ spontaneous dissociation, and for the $\text{CO}^{2+} \rightarrow \text{C}^+ (+ \text{O})$ process induced by collisions with argon (intense central peak only, see Fig. 4).

peaks studied in this way. (The data for the collision induced peak shown in Figs. 5 and 6 were even less reliable than the others, and are not shown in Fig. 9; however they also gave an identical onset, but with a larger uncertainty.) The reproducibility of these appearance energies in the present work (Fig. 9) is of the order ± 0.5 eV. This does not include any possible systematic error arising from differing shapes of the ionization efficiency curves near threshold.²⁰

IV. DISCUSSION

A. The unimolecular process

The fact that a diatomic ion is observed to spontaneously dissociate, with a lifetime in the microsecond range, must imply a predissociation mechanism as originally suggested.¹ Since so little is known^{9,10} about the electronic states of CO^{2+} , the nature of the barrier and thus of the predissociation mechanism must necessarily be speculative. However, as emphasized previously,^{8,11} the intrinsic form of the potential energy curves for a doubly charged diatomic species increases the probability that an electronically adiabatic mechanism (i.e., *not* Herzberg's case I) will be responsible for the predissociation. Most of the following discussion is based on the assumption that the mechanism involves tunneling through the potential barrier of the ground state.

A potential curve for the ground electronic state of CO^{2+} , computed previously,¹² is included in Fig. 1 in order to give some idea of its disposition relative to the states of CO^+ . However, the question of the states of CO^{2+} will now be considered in more detail. As mentioned above, the only

knowledge of these states comes from an ingenious procedure due to Hurley¹¹ which relates known spectroscopic states of a neutral diatomic (e.g., BN) to those of the isoelectronic doubly charged species (e.g., CO^{2+}). Two states of BN ($X^3\Pi$ and $A^3\Pi$) have been characterized spectroscopically,²¹ and three other states have been investigated²² by theoretical calculations. The term values and spectroscopic constants, both calculated and experimentally determined where available, have been conveniently tabulated.²² In order to generate Morse curves for these states, the dissociation energies must be known. The dissociation energy of the ground state of BN is the subject of some controversy, as described below. For reasons explained below, two sets of curves have been generated, one assuming $D_e = 5.0$ eV for the $X^3\Pi$ state of BN, the other assuming a value of 6.0 eV. The first of these values was used previously in the original work by Hurley,¹² who considered only the spectroscopically observed states of BN, and later by Hirsch *et al.*²³ who considered all five states. As pointed out previously,^{12,23} the resulting potential curve thus generated for the $X^3\Pi$ state of CO^{2+} , lies some 1.6 eV *above* the lowest vibrational level assigned,^{11,14} to this same state in the Auger spectrum¹⁴ of CO. This assignment was confirmed²⁴ by more recent Auger experiments which used both electron impact and Al K_α radiation to excite the Auger spectra; comparison of the two sets of data permitted²⁴ separation of the "normal" Auger spectra from high-energy satellite bands due to processes such as autoionisation of a neutral species excited by electron impact. While this more recent work²⁴ did not use energy resolution sufficiently high to resolve the vibrational structure observed previously,¹⁴ the onset of the appropriate carbon Auger band ($B - 1'$ in Table IV of Ref. 24) agrees well with the highest-energy resolved vibrational peak in the appropriate region (line 14 in Table 5.2.8 of Ref. 14). The agreement between carbon and oxygen Auger data is only moderate in each case^{14,24} (approximately 0.6 eV difference in the case of the observed onsets²⁴ for carbon and oxygen, respectively), but the potential curve calculated previously^{12,23} for the ground state of CO^{2+} is still too high by more than 1 eV.

The calculations reported previously,^{12,23} assuming a value of 5.0 eV for D_e for the $X^3\Pi$ state of BN, were repeated here, and are shown in Fig. 10(a); these curves appear to be identical with those published previously. The calculations were then repeated, using a value of 6.0 eV for $D_e(\text{BN})$, and the results are shown in Fig. 10(b). The curve for the $X^3\Pi$ ground state is now in more satisfactory agreement with the Auger data.^{14,24} In addition, the potential energy maximum, through which the observed tunneling is presumed to occur, is now in good agreement with the range of energies predicted by combining the known energy of the dissociation products with the present value (5.3 ± 0.1 eV) for the kinetic energy release. The previously reported value⁶ of kinetic energy release is some 0.5 eV higher, but it is not clear exactly how it was measured from the observed cutoff curves. In addition, no mention was made⁶ of any correction for the energy width of the main beam; judging from the published spectra,⁶ the latter appears to have been an appreciable fraction of the width of the metastable peak. Such a correction

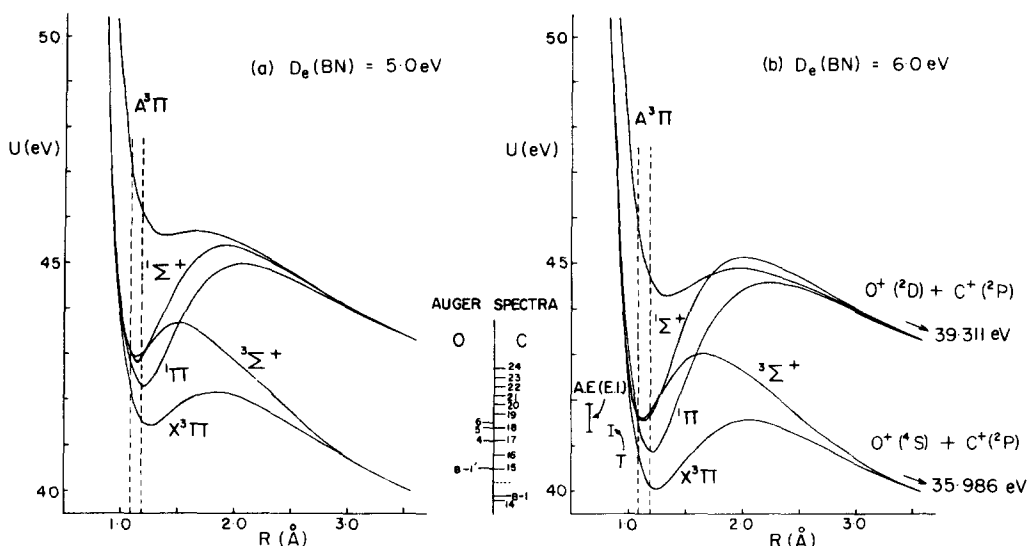
POTENTIAL ENERGY CURVES FOR CO^{2+} CALCULATED BY METHOD OF HURLEY FROM SPECTROSCOPIC DATA FOR BN.

FIG. 10. Semiempirical potential curves for states of CO^{2+} calculated by method of Hurley (Ref. 10) from spectroscopic constants (Refs. 21 and 22) for BN. Auger lines numbered 4–6 and 14–24 are from Siegbahn *et al.* (Ref. 14) and those labeled B–1' are onsets obtained by Moddeman *et al.* (Ref. 24). The kinetic energy release T is that determined in the present work, plotted relative to the dissociation limit of the $X^3\Pi$ ground state. The electron impact appearance energy is a composite of four independent determinations (Refs. 6, 7, 18 and 19). The dashed vertical lines give the Franck–Condon region for transitions out of the $\nu = 0$ level of the $X^1\Sigma^+$ state of CO. The curves shown in (a) were reported previously (Refs. 11 and 23).

would bring the earlier result⁶ into better agreement with that reported here.

The one remaining problem with the quantities represented in Fig. 10 involves the appearance energy of CO^{2+} measured by electron impact^{6,8,18,19} methods to be approximately 1.5 eV higher than the value obtained from Auger spectra.^{14,24} This discrepancy is well outside the combined uncertainties associated with repeatability of the measurements. Figure 10 suggests that Franck–Condon transitions should reach the lowest vibrational levels of the $X^3\Pi$ state of CO^{2+} , so that the discrepancy is not explicable on this basis if these potential curves are reliable. It is possible that the discrepancy is another example of well-known problems^{20,25} with estimating appearance energies from data obtained using unfiltered electron beam. As an example of the kind of internal ambiguities in the electron-impact data, one can cite the observation by one group⁸ of a distinct break in the ionization efficiency curve, corresponding to a second ionization energy of 45.9 eV; this feature was not observed in any other of the investigations.^{6,18,19} Another observation which, if valid is of great potential significance, is the equality⁶ of the appearance energies of CO^{2+} and of the fragment ions formed from metastable CO^{2+} . This result was confirmed in the present work (Fig. 9) but the observed signals are so weak that we consider it doubtful that the true threshold region was investigated by us. Thus, the fact that the slopes of the ionization efficiency curves (Fig. 9) are also indistinguishable from one another is suspicious, since simple considerations of fragmentation kinetics^{20,25} indicate that they should differ.

On the other hand, other evidence to be considered supports the contention that these appearance energy measurements are valid. Closely associated with the question of appearance energy is that of ion lifetime with respect to

dissociation. If the observed appearance energy^{6,8,18,19} of 41.6 eV, for both CO^{2+} and its fragments,⁶ is correct, and if the Auger data^{14,24} are also essentially correctly interpreted, then the potential curves for the $X^3\Pi$ state shown in Fig. 10 must be wrong. The true curve must be such that the Franck–Condon factors dictate that only vibrational levels near the energy of the potential energy maximum in the $X^3\Pi$ potential curve, including the predissociating levels, can be populated by electron impact. This would require that Franck–Condon restrictions do *not* apply to the net process $\text{CO} \rightarrow \text{CO}^{2+}$ occurring either in the Auger experiments,^{14,24} or in electron impact, or both. This could come about via vibrational readjustment in the primary CO^+ ion formed by loss of a K -shell electron, before the Auger process itself occurs. There is some evidence²⁶ in the case of N_2 that Auger transition time can be of the same order as vibrational periods. Alternatively, the Auger transitions could be vertical, while those induced by electron impact would then deviate from the Franck–Condon principle. At any rate, the discrepancy evident in Fig. 10, if real, leads one to predict that the reactivities with respect to dissociation, of CO^{2+} formed by Auger processes or by electron impact in the usual mass spectrometric energy range, should be qualitatively different. This is exactly what was found by Hirsch *et al.*²³ in a unique experiment designed to measure dissociative lifetimes of CO^{2+} formed either by electron impact at 150 eV or Auger transitions (Al K_α x rays). The data from the electron impact experiment could be fitted about equally well by assuming either 70% of the ions have a half-life of 9 μs with 30% having effectively infinite ($> 10^{-4}$ s) lifetime, or else a 16 μs half-life with no infinite lifetime component. On the other hand, the CO^{2+} ions formed by Auger transitions induced by x rays were not observed²³ to dissociate at all.

It thus seems clear²³ that the states of CO^{2+} reached

predominantly by electron impact in a mass spectrometer are qualitatively different from those observed in Auger spectra. The dissociative lifetimes of CO²⁺ produced by electron impact in a mass spectrometer were investigated previously by Newton and Sciamanna,⁶ who concluded that the half-life fell in the range 15–30 μ s, with zero contribution from infinite lifetime ions. However, the range of transit times (i.e., reaction times) available in the instrument used²⁷ ranged from about 1.5 μ s to less than 10 μ s, i.e., kinetic data were available⁶ for considerably less than one half-life. It is a standard exercise in phenomenological chemical kinetics²⁸ to show that even the order of reaction cannot be determined with any certainty unless data are available for times considerably in excess of a single half-life. In the present context, this translates into a lack of certainty in determining whether or not more than one process, with different lifetimes, contribute; this uncertainty is intrinsic, and is responsible for the ambivalent conclusions reached by Hirsch.²³ No such experiments were conducted in the present work, for precisely this reason, but one observation does pertain to the question of whether or not the CO²⁺ ions formed by electron impact include some appreciable fraction with effectively infinite lifetime. It was consistently observed that, on introducing collision gas to induce the central peak (Figs. 3 and 4), the intensity of the peak corresponding to unimolecular fragmentations of CO²⁺ was hardly affected. This was true certainly for all N₂, H₂, and Ar used as collision gases, even at pressures sufficiently high that the collision-induced peak was more intense than that arising from unimolecular dissociation. (The case of helium collision gas was less clearcut in this regard.) This suggests that the CO²⁺ ions responsible for the unimolecular processes are different from those from the collision-induced process, i.e., there must exist in the mass spectrometer a significant population of CO²⁺ ions with ef-

fectively infinite lifetimes for unimolecular dissociation. For this reason, we support the first alternative conclusion of Hirsch *et al.*²³ concerning CO²⁺ ions formed by electron impact, viz., half-life of 9 μ s or so, with about 30% of the CO²⁺ ions having a lifetime $> 10^{-4}$ s.

The discussion of the unimolecular dissociation of CO²⁺ has thus far been based upon the assumption that the predissociation mechanism responsible is an electronically adiabatic mechanism (Herzberg case 3) from rotational-vibrational levels of the ground electronic state. Energies and lifetimes of the vibrational levels ($v = 0$ to $v = 6$) calculated for the $X^3\Pi$ ground state correlating with the corresponding state of BN, assumed to have $D_e = 5.0$ eV [Fig. 10(a)], have been published previously.²³ Rotational quantum numbers $J = 0$ and $J = 7$ were considered,²³ and both of these rotational states with $v = 5$ were shown²³ to have lifetimes of the same order of magnitude as the mass spectrometer metastable window. In the present work, the potential curve for the $X^3\Pi$ state of CO²⁺, shown in Fig. 10(b), was similarly analyzed using a program developed by Leroy.²⁹ In all, more than 1400 vibrational-rotational states were located, and their widths and lifetimes estimated. It is not realistic to reproduce all of these here, and Table I lists energies and lifetimes for selected (v, J) combinations. In order to be a likely candidate for the predissociating state responsible for the unimolecular process observed (Fig. 2), a given rotational-vibrational state must have a lifetime not too far from the "metastable window" for the mass spectrometer used ($\sim 10^{-6}$ s), and in addition must have a J value corresponding to a rotational state which is appreciably populated in the CO neutral precursor at 200 °C. (This latter condition assumes that the formation of CO²⁺ by electron impact does not result in appreciable rotational excitation; all of the 12 lowest vibrational levels were found to have rotational levels

TABLE I. Energies and lifetimes of rotational-vibrational states of $X(^3\Pi)$ state of CO²⁺, assumed to be described by Hurley (Ref. 10) correlation: $E(R) = 35.986 + (14.399/R) - (1.4135 \times 6.00)[2e^{-\alpha} + e^{-2\alpha}]$, where $\alpha = [(1.1889R - 1.281) \times 2.0715]$.

Energies of $J = 0$ states							
v	0	1	2	3	4	5	6
E_v (eV)	40.115	40.261	40.401	40.537	40.666	40.790	40.909
	7	8	9	10	11	12	13
	41.020	41.126	41.224	41.315	41.398	41.470	41.527
Energies and lifetimes of states with lifetimes in range 10^{-5} – 10^{-7} s, with $J \leq 40^a$							
Vibrational level $v = 10$							
J	30	31	32	33	34	35	36
E (eV)	41.449	41.458	41.467	41.477	41.486	41.496	41.506
Lifetime (μ s)	9.19	5.37	3.10	1.76	0.99	0.55	0.31
	37						
E (eV)	41.516						
Lifetime (μ s)	0.17						
Vibrational level $v = 11$							
J	0	1	2	3	4	5	6
E (eV)	41.398	42.398	41.399	41.399	41.400	41.402	41.403
Lifetime (μ s)	1.44	1.42	1.37	1.30	1.22	1.12	1.01
	7						
E (eV)	41.405						
Lifetime (μ s)	0.90						
J	9	10	11	12	13	14	15
E (eV)	41.410	41.413	41.416	41.419	41.423	41.427	41.431
Lifetime (μ s)	0.67	0.57	0.47	0.39	0.31	0.25	0.19
	16						
E (eV)	41.435						
Lifetime (μ s)	0.15						
	17						
E (eV)	41.440						
Lifetime (μ s)	0.11						

^a For $J > 40$, population of rotational state of $v = 0$ level of $X^1\Sigma^+$ state of CO, at 200 °C, is less than 0.05% of population of $J = 10$ state.

with lifetimes of the appropriate order of magnitude but for $v = 0$, e.g., J has to be of the order of 120.)

Table I shows that the most likely candidates for the predissociating levels are $v = 10$ ($J = 30$ to 37) and $v = 11$ ($J = 0$ to 17), with the latter being more probable on the basis of the rotational populations of the CO precursor. In any event, all of the states have energies in the range 41.4–41.5 eV, in good agreement with the present observation (Fig. 2) of a narrow distribution of kinetic energy release from a state at 41.3 ± 0.1 eV. The states with $v = 12$ and $v = 13$ all had lifetimes much too short to correspond to the experimental time scale. It is noted that the larger number of vibrational levels supported by the $X^3\Pi$ potential function with the deeper well [Fig. 10(b)] is also in better qualitative agreement with the number of levels inferred to exist from the Auger spectrum.¹⁴

The only realistic predissociation mechanism, apart from that discussed so far, is one involving electronic curve crossing (case 1 of Herzberg⁹). While the potential curves of Fig. 10 can be taken as only a rough guide in this regard, it is clear that the general effect of the dominant Coulombic repulsion contribution will be to crowd the states together. Predissociation of excited states dissociating to excited fragments such as $\text{C}^+(^2P) + \text{O}^+(^2D)$, by states dissociating to ground state fragments, appears quite feasible. Excited triplet states probably radiatively decay to the $X^3\Pi$ ground state on a time scale short compared to that on which dissociation was observed in the present work, but this will not be true for the singlet states. The same selection rules⁹ apply to both emission and predissociation, and it is presently a matter for conjecture as to whether the $^1\Pi$ state shown in Fig. 10, e.g., might be predissociated by the $^3\Pi$ ground state on an appropriately slow time scale. The singlet–triplet transition is “forbidden,”⁹ but this could imply merely a slow process, e.g., microseconds. Certainly the energetic constraints, imposed by the observed appearance energies and kinetic energy release, are consistent with such a proposal [Fig. 10(b)]. Experimental evidence exists¹⁹ which shows that, on a time scale extending from essentially zero to about $3 \mu\text{s}$, CO^{2+} produced by electron impact dissociates with values of kinetic energy release ranging up to 22 eV. This must correspond to dissociation of CO^{2+} from excited electronic states, but it does not seem possible to draw any more detailed conclusions from this evidence.¹⁹ In general, the suggestion that electronic predissociation is responsible for the observed unimolecular dissociation of CO^{2+} can presently be neither proven nor disproven, due to lack of evidence.

B. Collision induced processes

The collision-induced processes observed in the present work fall naturally into two categories. Those involving a relatively small kinetic energy release, observed in the ion kinetic energy spectrum between the two horns arising from the unimolecular dissociation of CO^{2+} , correspond to processes (3) and (4) proceeding via process (2). The second category corresponds to process (5), and are observed with large kinetic energy release. This second category was observed at reasonable intensity only when helium was used as collision gas.

The nondissociative process (2) was confirmed in the present work via $2E$ spectra.¹⁵ The energetics of this process are such that

$$\Delta E_{\text{exc}}(\text{CO}^+) + \Delta E_{\text{exc}}(\text{M}^+) = 26.5 \text{ eV} - IE(\text{M}) + Q, \quad (6)$$

where ΔE_{exc} represents internal excitation energy, the difference between second (Auger values^{14,24}) and first ionization energies of CO is 26.5 eV, and Q represents any kinetic energy loss transformed to internal energy by the collision. For the cases $\text{M} = \text{Ar}$, N_2 , or H_2 , the values of $IE(\text{M})$ all fall in the range 15.5–15.9 eV, so that in the absence of any kinetic energy loss Q the total excitation energy available is 10.5–11 eV. For the case of $\text{M} = \text{He}$ this excitation energy is only 2 eV, so that an appreciable contribution from Q is necessary if the same processes are to be observed. The fact that the nondissociative process (2) was observed in good yield must correspond to collisions in which most of the excitation energy is deposited in M^+ . Alternatively, some of the excitation energy could be dissipated radiatively, as has been observed³⁰ in collisions of CO^{2+} with H_2 .

First the case where $\text{M} = \text{Ar}$, N_2 , or H_2 will be discussed. All of these give collision induced spectra like Fig. 4, with what appears to be vibrational structure. This vibrational structure could correspond either to that of the CO^{2+} , in which case the CO^+ ions which dissociate must presumably be formed on a repulsive curve, or else the structure corresponds to that in a bound state of CO^+ which is predissociated by some mechanism to be determined. The structure observed experimentally (Fig. 4) corresponds to a vibrational spacing of about 0.18 eV. This is a little larger than that calculated for the lowest vibrational levels of CO^{2+} (Table I) using the larger value for the dissociation energy, or indeed than that calculated previously²³ using the lower value for $D_e(\text{BN})$. However, the status of these calculations based on Hurley's method¹¹ is such that no great weight can be placed upon this discrepancy. Unfortunately almost nothing is known about states of CO^+ which are repulsive in the appropriate range of internuclear distance R . The available information has been summarized by Smyth *et al.*³¹ who investigated dissociative excitation of neutral CO from high-Rydberg states; such experiments^{31,32} are usually interpreted in terms of an ion-core model, in which the Rydberg electron acts as spectator to the dissociation of the CO^+ core. The $C^2\Delta_r$ state of CO^+ has been reasonably well characterized spectroscopically,³³ and with a fairly large value of $R_e = 1.346 \text{ \AA}$ is known to be repulsive over an interesting range of values of R (Fig. 1). The only other experimental evidence concerning the repulsive states of CO^+ , sufficiently complete that a potential curve could be proposed, concerns³⁴ the velocity distribution of C^+ arising from collision induced dissociation of CO^+ . This repulsive state³⁴ lies so close to the repulsive portion of the $C^2\Delta_r$ state that it could not be clearly plotted in Fig. 1; it seems likely that Moran *et al.*³⁴ were able to infer at least the repulsive portion of the C state from their work on collision induced dissociation before the spectroscopic information³³ was available, a remarkable achievement.

The curves drawn for the D , E , and F states in Fig. 1 are

particularly uncertain. Photoelectron spectra^{41,42} and photoionization absorption spectra⁴¹ showed well-defined progressions. The electronic transitions giving rise to these progressions were interpreted satisfactorily with the aid of INDO/CI calculations.⁴³ However, vibrational state numbering could not be unambiguously assigned and no rotational structure could be resolved^{41,42} permitting estimates of bond lengths. The curves shown in Fig. 1 for these D , E , and F states are Morse curves for which the parameters were derived by the following very approximate procedure. The observed^{41,42} vibrational lines were assumed to correspond to $v = 0, 1, 2$, etc. This permitted estimation of a vibrational frequency and of a value of D_e , and thus a value of the Morse parameter β . The vertical ionization energies to these states are given,⁴² and these must correspond to the transition with the maximum overlap between the $v = 0$ level of the $X^1\Sigma^+$ state of CO and the appropriate vibrational level of the upper state. It was assumed that this transition corresponds to a transition at a value of $r = r_e$ for the $X^1\Sigma^+$ state of CO , and that this corresponds to the inner turning point for the appropriate vibrational level of the upper state. Together with the values for D_e and β , this permitted an estimate of r_e for the upper state. Clearly, these curves drawn (Fig. 1) for the D , E , and F states must be considered with considerable reserve, though their general dispositions with respect to both energy and bond length must be approximately correct.

Quite apart from these uncertainties in the potential curves for stable CO^{2+} and for dissociative CO^+ , there is the question of the applicability of the Franck-Condon principle in these charge-exchange collisions. Thus, formation of CO^+ in the $B^2\Sigma^+$ state, via collisions of CO^{2+} with H_2 , was observed³⁰ via the CO^+ ($B \rightarrow X$) emission bands. The observed spectra could not be accounted for³⁰ using the $^3\Pi$ ground state parameters for CO^{2+} calculated previously^{12,23} [Fig. 10(a)] and the well-established parameters^{9,10} for the B state of CO^+ . While the spectroscopic constants for CO^{2+} are clearly suspect, the possibility of nonconformance with the Franck-Condon principle in the charge transfer step was also mentioned.³⁰ In fact, such nonvertical transitions appear³⁵⁻³⁷ to be well established for charge exchange collisions between Ar^+ (and other ions) and neutral CO , to form predominantly CO^+ ($A^2\Pi$). This deviation can be well explained by a model³⁵ which takes into account the polarization of the CO molecule in the vicinity of the Ar^+ ion. Alternatively, essentially the same physical idea may be expressed³⁶ in terms of the potential energy surfaces of the initial and final states, of the system of three colliding particles, coming close together or even intersecting. This is in essence identical with ideas proposed by Durup³⁸ for non-vertical dissociative collisions (designated³⁸ process 1-2), although the observable consequences are somewhat different than in the case of emission.

Thus, the proposal that the vibrational structure evident in Fig. 3 corresponds with that in the CO^{2+} ion is beset with ambiguities in the available subsidiary information required to test it. While this proposal is thus by no means excluded, it appears possible to offer a rather satisfactory account of Fig. 4 in terms of the alternative hypothesis, viz. that the vibrational structure corresponds to that in a predissociated state of CO^+ .

Predissociations in CO^+ have been extensively investigated by Locht,^{39,40} using a unique apparatus incorporating controlled energy electron impact combined with kinetic energy analysis of the product ions. A dissociation channel leading to $\text{C}^+ + \text{O}$, with an onset at 22.35 eV, was observed^{39,40} to occur with a vibrational structure very similar to that of Fig. 4. In turn, this structure^{39,40} was shown to correspond closely to that observed^{41,42} in a particular progression in the photoelectron spectrum of CO , also observed⁴¹ in the absorption spectrum near 550 Å. The progression of interest here (fourth photoelectron progression^{41,42}) was interpreted in terms of a transition to a $D^2\Pi$ state of CO^+ which dissociates to $\text{C}(^3P) + \text{O}(^4S)$ fragments. However, this $D^2\Pi$ state is predissociated^{39,40} by the $C^2\Delta$ state,³³ which dissociates to give $\text{C}^+(^2P) + \text{O}(^3P)$ i.e., ground state fragments at 22.37 eV above the ground state of CO , in good agreement with the observed^{39,40} onset. This is also well within the range of energies available in the charge transfer process [Eq. (6)] of CO^{2+} with Ar , N_2 , or H_2 . The intense central peak (Fig. 4) could correspond to direct transitions to the $C^2\Delta$ state. The corresponding process (4) forming O^+ requires an energy at least 24.73 eV above the $v = 0$ level of the ground state of CO , if ground state fragments $\text{C}(^3P) + \text{O}(^4S)$ are to be formed; as seen in Fig. 8, this process is of much lower intensity than is the competing process (3), for $M = \text{Ar}$, N_2 , H_2 .

For the case of $M = \text{He}$, where only 2 eV of excitation energy is available [Eq. (6)] for the CO^+ ion, qualitatively different spectra are observed. Thus, the C^+ fragments formed via process (3) with lower values of kinetic energy release (Fig. 7) appear to arise from two dissociating states of CO^+ which, to be reached, require different values of kinetic energy loss Q . Since measurement of kinetic energy loss is a direct measurement, with no advantage of an "amplification factor" which assists in measurements of kinetic energy release,¹⁵ the low signal-to-noise ratio and poor energy resolution apparent in Fig. 7 make such measurements particularly unreliable. The poorly resolved peak at lower values of V/V_0 appears very close to the position predicted if the kinetic energy loss were zero. The other peak corresponds to a kinetic energy loss of about 25 eV, but the uncertainty in each of these estimates is of the order of 15 eV. Interpretation must necessarily be speculative, but it is possible that the former peak corresponds to collision-induced dissociation of ground state CO^+ (vibration-rotational excitation only) while the peak corresponding to an appreciable kinetic energy loss corresponds to dissociation via excitation either the E or F state (Fig. 1).

Helium is considerably more efficient, than any other of the collision gases used, in producing O^+ from process (4). Two states of CO^+ which dissociate to O^+ are known from photoelectron spectroscopy,^{41,42} the $D^2\Pi$ and $E^2\Sigma^+$ states at about 22.7 and 25.4 eV above the ground state of CO , respectively. If either of these is the state responsible for Fig. 7, the values of Q required to reach their $v = 0$ vibrational levels would be about 7 and 9.5 eV, respectively; the assigned⁴⁰ dissociation limits lie at 24.73 and 28.05 eV, respectively, i.e., more than 2 eV higher still.

Finally, the spectra shown in Fig. 5 and 6 can be briefly

discussed in terms of process (5). Again, helium is by far the most efficient collision gas in this regard. The values of kinetic energy release deduced from the C^+ and O^+ spectra (Figs. 5 and 6, respectively) agree with one another, as they should if states of CO^{2+} are responsible. The subsidiary maxima in the curves correspond to a kinetic energy release of 7.9 eV, in good agreement with the maximum in the kinetic energy distribution observed by Brehm and Frenes¹⁹ immediately following electron impact of CO. These latter experiments involve a time scale from effectively zero to 3 μs , and thus sample much shorter-lived (and presumably more energetic) CO^{2+} ions than do the present investigation of unimolecular dissociation of CO^{2+} . However, the processes induced by collision with He presumably sample at least some of the states responsible for the earlier observation.¹⁹ The maximum kinetic energy release for process (5) induced by collisions with helium was about 13 eV (Figs. 5 and 6), compared with about 22 eV observed previously.¹⁹

V. CONCLUSIONS

(i) The predissociation process responsible for the unimolecular dissociation of CO^{2+} on the microsecond time scale is most likely an example of predissociation case III of Herzberg,⁹ as suggested previously.^{6,7,12} The semiempirical potential curves for the states of CO^{2+} , calculated by Hurley,¹² have been recalculated with a larger dissociation energy; these revised curves better correlate data from Auger spectra, appearance energies, and kinetic energy release. However, the possibility that a case I predissociation⁹ is responsible cannot be ruled out entirely.

(ii) The most efficient collision-induced dissociation process involved charge transfer as a primary step, from collision gases of sufficiently low ionization energy that appreciable excitation energy (> 10 eV) was available to the products of the charge-transfer process. The most probable mechanism involves predissociation (Herzberg case I) of the $D^2\Pi$ state of CO^+ by the $C^2\Delta$ state to yield $\text{C}^+(^2P)$ fragments (the inherent width of the lines observed in the photoelectron spectra⁴² would preclude observation of predissociation broadening in these spectra. This is not necessarily so for the absorption spectra,⁴¹ however). The channel leading to O^+ was much less efficient. This collision-induced process did not appear to compete with the spontaneous dissociation process suggesting that the beam of CO^{2+} contained an appreciable fraction of ions which were *not* metastable on the instrumental time scale.

(iii) When helium was used as collision gas, dissociation via charge transfer was still observed. However, the overall efficiency was considerably less than with Ar, N_2 , or H_2 , and production of O^+ was appreciably more efficient than the C^+ channel. There was clear evidence of appreciable kinetic energy loss contributing to the required energy, but no accurate measurements were possible in the present work.

(iv) Collision-induced dissociation of CO^{2+} , without charge transfer as a primary step, competed significantly with the unimolecular process only if helium was used as collision gas. Fragment ions with up to 13 eV of excess kinetic energy were detected.

(v) It would be advantageous to have these experiments,

particularly those involving appreciable kinetic energy loss, repeated on an apparatus capable of higher energy resolution, and also with adequate facilities for angular collimation. Use of collision gas with an ionization energy intermediate between that of helium and argon, e.g., neon, would be of interest. In the absence of direct spectroscopic observation of states of CO^{2+} , good modern calculations of these states would be desirable.

ACKNOWLEDGMENTS

The authors are indebted to R. J. Leroy for the calculations summarized in Table I. This work was supported by NSERC, Canada.

- ¹E. Friedlander, H. Kallmann, W. Lasareff, and B. Rosen, *Z. Phys.* **76**, 60 (1932).
- ²J. A. Hipple, *J. Phys. Colloid. Chem.* **52**, 456 (1948).
- ³C. E. Melton and G. F. Wells, *J. Chem. Phys.* **27**, 1132 (1957).
- ⁴S. E. Kupriyanov, *Sov. Phys. Tech. Phys.* **9**, 659 (1964).
- ⁵J. B. Hasted, *Physics of Atomic Collisions* (Elsevier, New York, 1972), 2nd ed.
- ⁶A. S. Newton and A. F. Sciamanna, *J. Chem. Phys.* **53**, 132 (1970).
- ⁷J. H. Beynon, R. M. Caprioli, and J. W. Richardson, *J. Am. Chem. Soc.* **94**, 1852 (1971).
- ⁸F. H. Dorman and J. D. Morrison, *J. Chem. Phys.* **35**, 575 (1961).
- ⁹G. Herzberg, *Spectra of Diatomic Molecules*, 2nd ed. (Van Nostrand, Princeton, 1950), pp. 405–437.
- ¹⁰K. P. Huber and G. Herzberg, *Spectroscopic Constants of Diatomic Molecules* (Van Nostrand, Princeton, 1979).
- ¹¹(a) A. C. Hurley and V. W. Maslen, *J. Chem. Phys.* **34**, 1919 (1961); (b) A. C. Hurley, *J. Mol. Spectrosc.* **9**, 18 (1962).
- ¹²A. C. Hurley, *J. Chem. Phys.* **54**, 3656 (1971).
- ¹³A. G. Gaydon, *Dissociation Energies and Spectra of Diatomic Molecules* (Chapman and Hall, London, 1968).
- ¹⁴K. Siegbahn, C. Nordling, G. Johansson, J. Hedman, P. F. Heden, K. Hamrin, U. Gelius, T. Bergmark, L. O. Werme, R. Manne, and Y. Baer, *ESCA Applied to Free Molecules* (North-Holland, Amsterdam, 1969), pp. 76–82.
- ¹⁵R. G. Cooks, J. H. Beynon, R. M. Caprioli, and G. R. Lester, *Metastable Ions* (Elsevier, Amsterdam, 1973).
- ¹⁶M. Barber and R. M. Elliott, 12th Conference on Mass Spectrom. Allied Topics, ASTM Committee E-14, Montreal, 1964, Paper No. 22.
- ¹⁷M. J. Lacey and C. G. Macdonald, *Org. Mass Spectrom.* **13**, 284 (1978).
- ¹⁸E. Hille and T. D. Mark, *J. Chem. Phys.* **69**, 4600 (1978).
- ¹⁹B. Brehm and G. DeFrenes, *Int. J. Mass Spectrom. Ion Phys.* **26**, 251 (1978).
- ²⁰R. K. Boyd and J. H. Beynon, *Int. J. Mass Spectrom. Ion Phys.* **23**, 163 (1977).
- ²¹A. E. Douglas and G. Herzberg, *Can. J. Res. Sect. A* **18**, 179 (1960).
- ²²G. Verhaegen, W. G. Richards, and C. M. Moser, *J. Chem. Phys.* **46**, 160 (1967).
- ²³R. G. Hirsch, R. J. van Brunt, and W. D. Whitehead, *Int. J. Mass Spectrom. Ion Phys.* **17**, 335 (1975).
- ²⁴W. E. Moddeman, T. A. Carlson, M. O. Krause, and B. P. Pullen, *J. Chem. Phys.* **55**, 2317 (1971).
- ²⁵J. H. Beynon, R. G. Cooks, K. R. Jennings, and A. J. Ferrer-Correia, *Int. J. Mass Spectrom. Ion Phys.* **18**, 87 (1975).
- ²⁶D. Stalherm, B. Cleff, H. Hillig, and W. Mehlorn, *Z. Naturforsch. Teil A* **24**, 1728 (1969).
- ²⁷A. S. Newton and A. F. Sciamanna, *J. Chem. Phys.* **52**, 327 (1970).
- ²⁸S. W. Benson, *The Foundations of Chemical Kinetics* (McGraw-Hill, New York, 1960).
- ²⁹R. J. Leroy (private communication).
- ³⁰G. H. Bearman, F. Ranjbar, H. H. Harris, and J. J. Leventhal, *Chem. Phys. Lett.* **42**, 335 (1976).
- ³¹K. C. Smyth, J. A. Schiavone, and R. S. Freund, *J. Chem. Phys.* **60**, 1358 (1974).

- ³²W. C. Wells, W. L. Borst, and E. C. Zipf, *Phys. Rev. A* **17**, 1357 (1978).
- ³³J. Marchand, J. D'Incan, and J. Janin, *Spectrochim. Acta Part A* **25**, 605 (1969).
- ³⁴T. F. Moran, F. C. Petty, and A. F. Hedrick, *J. Chem. Phys.* **51**, 2112 (1969).
- ³⁵M. Lipeles, *J. Chem. Phys.* **51**, 1252 (1969).
- ³⁶G. N. Polyakova, V. F. Erko, A. V. Zats, Ya. M. Fogel, and G. D. Tolstolutskaia, *Sov. Phys. JETP Lett.* **11**, 390 (1970).
- ³⁷D. Brandt, Ch. Ottinger, and J. Simonis, *Ber. Bunsenges. Ges.* **77**, 648 (1973).
- ³⁸J. Durup, *Recent Developments in Mass Spectrometry*, edited by K. Ogata and T. Hayakawa (University of Tokyo, Tokyo, 1970), p. 921.
- ³⁹R. Locht and J. M. Durer, *Chem. Phys. Lett.* **34**, 508 (1975).
- ⁴⁰R. Locht, *Chem. Phys.* **22**, 13 (1977).
- ⁴¹K. Codling and A. W. Potts, *J. Phys. B* **7**, 163 (1974).
- ⁴²L. Asbrink, C. Fridh, E. Lindholm, and K. Codling, *Phys. Scr.* **10**, 183 (1974).
- ⁴³M. Okuda and N. Jonathan, *J. Electron. Spectrosc. Relat. Phenom.* **3**, 19 (1974).
- ⁴⁴P. H. Krupenie and S. Weissman, *J. Chem. Phys.* **43**, 1529 (1965).